

Artificial Viruses and Their Application to Gene Delivery. Size-Controlled Gene Coating with Glycocluster Nanoparticles

Yasuhiro Aoyama,^{*,†} Takuya Kanamori,[†] Takashi Nakai,[†] Toshinori Sasaki,[†] Shohei Horiuchi,[†] Shinsuke Sando,[†] and Takuro Niidome[‡]

Department of Synthetic Chemistry and Biological Chemistry, Graduate School of Engineering, Kyoto University, Yoshida, Sakyo-ku, Kyoto 606-8501, Japan, and Department of Applied Chemistry, Faculty of Engineering, Nagasaki University, Nagasaki 852-8521, Japan

Received December 5, 2002; E-mail: aoyamay@sbchem.kyoto-u.ac.jp

Number-, size-, and shape-controlled macromolecular associations are common in biology. A typical example is viruses in which a single genetic molecule (DNA or RNA) is coated with a definite number of capsid proteins. Viruses are used as gene carriers (vectors)¹ in gene therapy,^{1,2} but their performance is still not satisfactory. Nonviral gene delivery relies on cationic amine vectors (polymers and lipid aggregates),^{3–16} where a common problem is difficulty in size control. Polycation–polyanion amine–DNA complexation often undergoes cross-link and further aggregation to give polynuclear (polymolecular in DNA)⁵ and huge particles,^{6,7} whose size-restricted poor diffusion severely limits their *in vivo* utility. There is also good evidence that endocytosis is highly size-dependent.⁸ “Artificial viruses” should be mononuclear, stoichiometric,⁹ of a viral size (≤ 100 nm), and capable of transfection. While detergent^{10,11} and saccharide¹² manipulation of cationic vectors allows mononuclear DNA to collapse into a viral size, we are concerned here about gene coating, as in real viruses, with spherical and neutral nanoparticles which are strongly adhesive on DNA but not with each other. A choice here is saccharide nanoparticles derived from macrocyclic glycocluster compound **1** (Scheme 1),¹⁷ which (**1b**) has been shown to interact with the phosphate ions of Na_2HPO_4 ^{18,19} and, in a preliminary form, DNA.²⁰ Now we wish to report here a novel example of artificial glycoviral vectors which meet the above criteria.^{21,22}

Reaction of octamine **1c** with cellobiose (4-*O*- β -D-glucopyranosyl-D-glucose) lactone affords compound **1a**²³ (molecular weight, 4172) having four long alkyl chains ($R = \text{undecyl}$) and eight saccharide moieties with receptor-inert β -glucoside termini on the opposite sides of the bowl-shaped calix[4]resorcinarene macrocycle (Scheme 1). Like its α -glucoside counterpart **1b**,¹⁹ cone-shaped, quadruple-chain glycocluster amphiphile **1a** in water forms micelle-like aggregates, hereafter called glycocluster nanoparticles (GNPs, Scheme 1 in a schematic form), which can be characterized by gel permeation chromatography (GPC, Figure 1a) as having a pullulan-calibrated total molecular weight of 22 000 and hence an aggregation number of ~ 5 ($n_{\text{agg}} = 22\,000/4172 \cong 5.3$) (Scheme 1), dynamic light scattering (DLS, Figure 1b) as having a size (diameter) of $d \cong 4$ nm, and also transmission electron microscopy (TEM) in accord with the GPC and DLS results (Figure 2a and b).²⁴

The interaction of glycocluster **1a** with 7040 bp (base pair) plasmid pCMVluc having a reporter gene for firefly protein luciferase and a cytomegalovirus promoter was monitored by agarose gel electrophoresis. The double-helical DNA (pCMVluc) becomes immobile in the presence of host **1a** at host/base or host/phosphate ratios of $\mathbf{1a/P} \geq 0.3$ and completely at $\mathbf{1a/P} \geq 0.5$ (Figure

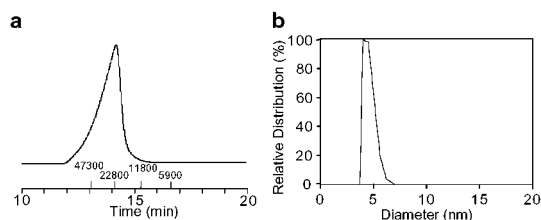
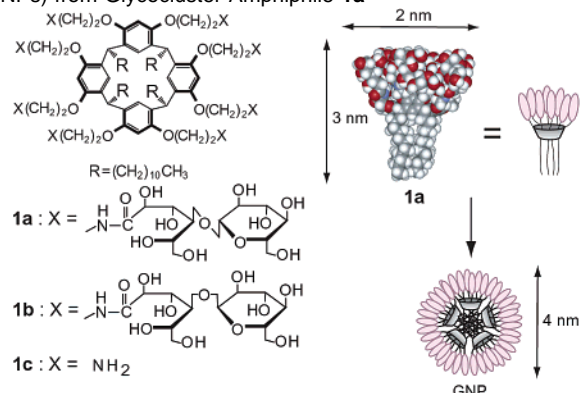


Figure 1. (a) Gel permeation chromatogram of **1a** with water as an eluent. The numbers 5900, 11 800, 22 800, and 47 300 refer to the elution positions of molecular-weight markers (pullulans) having respective molecular weights. (b) Size distribution of **1a** (1 mM) in water in reference to number of particles as evaluated by Gaussian analysis of dynamic light scattering data.

Scheme 1. Formation of Micellar Glycocluster Nanoparticles (GNPs) from Glycocluster Amphiphile **1a**



3a). DLS measurements indicate that cross-link occurs under conditions of $\mathbf{1a/P} \leq 0.4$ but saturation is reached at $\mathbf{1a/P} \cong 0.6$; the size of the resulting **1a**-pCMVluc complex remains nearly constant thereafter at ~ 54 nm (Figure 3b) in accord with the TEM image of the particles (40–70 nm) taken at $\mathbf{1a/P} = 0.7$ (Figures 2c,d and S1).²⁴ The surface (zeta) potential of the complex is negative in the presaturation region ($\zeta \cong -10$ mV at $\mathbf{1a/P} = 0.5$), where surface coverage of polyanionic DNA may be incomplete, but is rendered neutral after saturation with neutral GNPs ($\zeta \cong 0$ mV at $\mathbf{1a/P} = 1.0$ or 2.0). The saturation stoichiometry of $\mathbf{1a/P} \cong 0.6$ is equivalent to a $\mathbf{1a/bp}$ ratio of 1.2, indicating that 12 molecules of **1a** or ~ 2 GNPs ($n_{\text{agg}} = 5.3$) are bound in every helical pitch (10 bp) of pCMVluc.

Surface plasmon resonance²⁵ (SPR, Figure 3c) using a **1a**-immobilized sensor chip shows a slow but straight association (A) and horizontal dissociation (D) profile for pCMVluc, indicating that the strong and practically irreversible **1a**-pCMVluc complexation is driven by multiple hydrogen bonding between OH groups of host **1a** and phosphate groups of pCMVluc.²⁶ Such an interaction

[†] Kyoto University.
[‡] Nagasaki University.

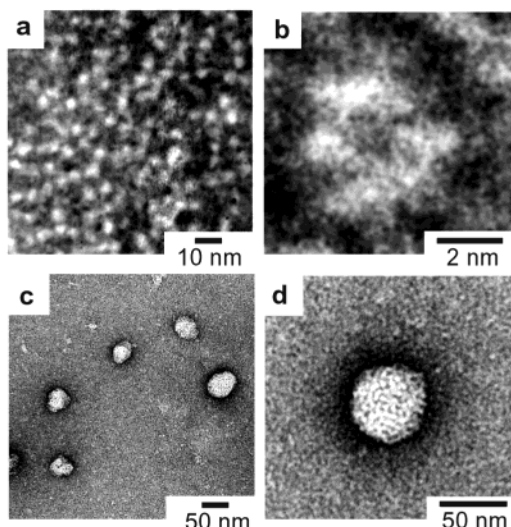


Figure 2. Transmission electron microscopic (TEM) images of GNPs and their complexes (glycoviruses) with pCMVluc in water with uranyl acetate (2 wt %) as a negative stainer. (a) GNPs with a size of ~ 4 nm as observed for a solution of **1a** (1.0 mM) in water. (b) Enlargement of a GNP, which appears to be composed of several molecules of **1a**. (c) **1a**-pCMVluc complexes (glycoviruses) with a size of ~ 50 nm as observed for a solution of pCMVluc (50 μ M P) and **1a** (35 μ M) at **1a**/P = 0.7. (d) Enlargement of a **1a**-pCMVluc complex (glycovirus).

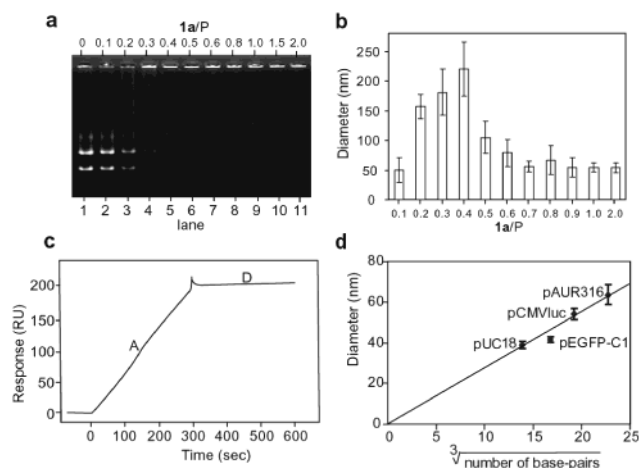
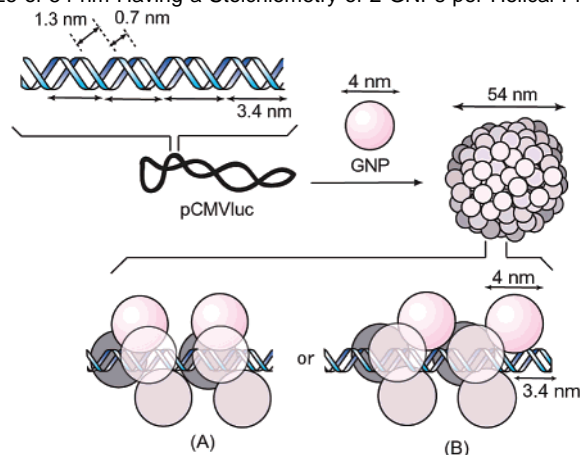


Figure 3. Complexation of **1a** with pCMVluc and other plasmid DNAs. (a) Electrophoretic gel shifts for pCMVluc in the absence (lane 1) and presence of increasing amounts (lanes 2–11) of **1a**, using 0.7% agarose gel in 40 mM Tris-acetate buffer. (b) Variation in the average sizes (for triplicate measurements) of **1a**-pCMVluc complexes arising from pCMVluc (1 μ M P) in the presence of increasing amounts of **1a** in HEPES buffer (10 mM, pH 7.4, [NaCl] = 150 mM). (c) Surface plasmon resonance (SPR) profile (RU = resonance unit) upon treatment of a **1a**-immobilized sensor chip, prepared in a manner similar to that of the **1b**-immobilized one (refs 19 and 25), with 100 μ L of a solution of pCMVluc (2.5 μ M P). (d) Correlation of average sizes (for at least quadruplicate measurements) of **1a**-plasmid complexes with cubic roots of numbers of base pairs under conditions of 1 μ M P for the plasmids at **1a**/P = 1.0.

would be maximized when GNPs ($d \cong 4$ nm) are aligned along the major groove (1.3 nm width and 3.4 nm pitch length) of DNA. Models indicate that 4 GNPs could be bound in two pitches without steric interference in one of two modes, A (4 GNPs in a pitch in every two pitches) and B (2 GNPs in every successive pitch, located at north and south or east and west pitch by pitch) (Scheme 2). The maximal accommodation of 2 GNPs per pitch is in fact the saturation stoichiometry observed. The characteristic contrast or fine structure of the glycoviral particle (Figure 2d)²⁴ may reflect GNP-coating of DNA (Scheme 2).

Scheme 2. Illustration of GNP-Induced Compaction of Supercoiled pCMVluc Plasmid DNA into a Glycoviral Particle of a Size of 54 nm Having a Stoichiometry of 2 GNPs per Helical Pitch



The saturation ratio of **1a**/P $\cong 0.6$ and the aggregation number of $n_{\text{agg}} = 5.3$ for GNP define the composition of the present glycoviral complex encapsulating 7040 bp plasmid pCMVluc as pCMVluc \cdot (~ 8450 **1a**) or pCMVluc \cdot (~ 1600 GNP). The volume of pCMVluc, assuming a cylinder with a cross-sectional diameter of 2.4 nm, is $V_{\text{DNA}} = \pi \cdot (2.4/2)^2 \cdot 3.4 \cdot (7040/10) = 10\,800$ nm³. That of 1600 spherical ($d = 4$ nm) GNPs with a void volume of 26% at closest packing would be $V_{\text{GNP}} = 1600 \cdot (4\pi/3) \cdot (4/2)^3 \cdot 0.74 = 72\,500$ nm³. The sum of these, that is, $V_{\text{DNA}} + V_{\text{GNP}} = 83\,300$ nm³, represents the lower limit of the volume of the complex and is very close to the real volume of the observed spherical glycoviral particle (Figure 2d) having a DLS size of $d = 54$ nm ($V_{\text{virus}} = (4\pi/3) \cdot (54/2)^3 = 84\,200$ nm³). Other plasmid DNAs such as pUC18 (2686 bp), pEGFP-C1 (4731 bp), and pAUR316 (11 663 bp) form respective glycoviral complexes whose DLS sizes show a cubic-root dependence, as referred to before,¹¹ on the base-pair numbers (Figure 3d). There is no doubt that the present glycoviruses contain a single DNA molecule as a template and are highly efficiently packed (Scheme 2 and Figure 2d), resulting in effective charge shielding ($\zeta \cong 0$ mV). It is remarkable that the otherwise nonadhesive GNPs are closely packed when aligned on the DNA template and that the resulting glycoviruses coated with GNPs are again rendered nonadhesive²⁷ to keep monomolecularity in a wide range of **1a**/P after saturation (Figure 3b). More or less hydrophobic particles, on the other hand, tend to aggregate upon charge neutralization.¹³

The last or the most critical criterion for artificial viral vectors after monomolecularity, stoichiometry, and size is transfection ability. The glycoviral particles pCMVluc \cdot (~ 1600 GNP) effectively transfect HeLa cells and other (CHO, Huh-7, HepG2, and COS) cells as well in a serum-free medium and more effectively (by a factor of 50–100%) in the presence of fetal bovine serum (10%). The serum-free transfection efficiencies (Figure 4a, red bars) are roughly constant in the saturation range (**1a**/P = 0.6–2.0) and are approximately an order of magnitude higher than that of lipofectin (L),¹⁴ a standard cationic-lipid vector. The glycoviruses are not cytotoxic, although excess GNPs seem to be slightly so, so that cell viabilities fall down to $\sim 85\%$ at higher **1a**/P (Figure 4a, black dots). Transfection of pEGFP-C1-containing glycoviruses, included in the correlation in Figure 3d, also results in effective expression of encoded green fluorescent protein (Figure 4b).

The generally accepted role of amine/ammonium vectors in gene delivery is multifold. As ammonium cations, they bind to polyanionic DNAs and also to negatively charged cell surfaces¹⁵ to trigger endocytosis. As free-base amines, they serve as “proton

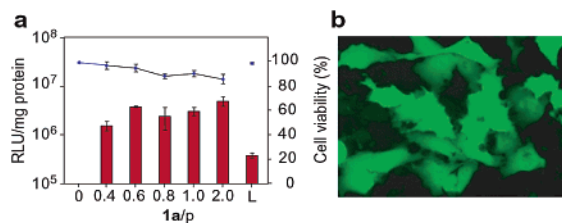


Figure 4. Transfection of HeLa cells with glycoviruses pCMVluc (~1600)-GNP. (a) Luciferase expression efficiencies (red bars) in terms of chemiluminescence (luciferin/ATP/O₂) relative light units (RLU) per mg of total protein in the cells (<10³ at 1a/P = 0) and cell viabilities (black dots) in reference to that of control (100% at 1a/P = 0) for triplicate runs as functions of 1a/P. Transfection conditions: cells (80–90% confluent), pCMVluc (15 μM P), and 1a (1a/P = 0–2.0) in a serum-free medium (50 μL) in a 96-well plate at 37 °C for 3 h and further for 48 h in a new medium (200 μL) containing fetal bovine serum (10%). L represents control runs using lipofectin under optimized conditions. (b) Fluorescence micrograph of HeLa cells transfected with glycoviruses containing plasmid pEGFP-C1 having a reporter gene for green fluorescent protein (GFP).

sponges¹⁶ and promote endocytic membrane disruption to liberate the DNA. The present results clearly show that these amine/ammonium-characteristic functions are by no means the prerequisites of artificial vectors. The intrinsic function of viruses, that is, cell invasion followed by gene expression, seems to be also intrinsic to size-manipulated artificial viruses, although the role of coating saccharide clusters in cellular communications remains to be uncovered.

In conclusion, the GNP-pCMVluc complexation gives rise to viruslike particles which are compactly packed, are well charge-shielded, and efficiently transfect cell cultures, thus opening a new (nonamine/noncationic/nonpolymeric) strategy of less cytotoxic and serum-compatible gene delivery. The viruses are a typical case where a definite number of macromolecules are assembled into a harmonious whole. Topologically programmed metal coordination²⁸ may be taken as an abiological example of number-controlled multimolecular associations. The present glycoviruses, although by no means monodispersed (Figures 1, 2c, 3b, and S1), provide a new approach to number and size control in functional macromolecular oligomerization.²⁹ The hierarchical growth of glycocluster amphiphile 1a through GNP to transfecting glycoviral particle reveals a remarkably manipulated adsorption performance of the saccharide clusters to keep the integrity of GNPs, to control intraviral compaction while preventing interviral fusion, and to promote cell-virus adhesion.

Acknowledgment. This work was supported by RFTF of JSPS, by Grant-in-Aids for COE Research and Scientific Research from the Japanese government, and also by CREST of JST.

Supporting Information Available: Figure S1 (PDF). This material is available free of charge via the Internet at <http://pubs.acs.org>.

References

- Wilson, J. M. *N. Engl. J. Med.* **1996**, *334*, 1185–1187.
- (a) Verma, I. M.; Somia, N. *Nature* **1997**, *389*, 239–242. (b) Anderson, W. F. *Nature* **1998**, *392*, 25–30.
- (a) Behr, J.-P. *Acc. Chem. Res.* **1993**, *26*, 274–278. (b) Nishikawa, M.; Huang, L. *Hum. Gene Ther.* **2001**, *12*, 861–870. (c) Zuber, G.; Dauty, E.; Nothisen, M.; Berguise, P.; Behr, J.-P. *Adv. Drug Delivery Rev.* **2001**, *52*, 245–253. (d) Gebhart, C. L.; Kabanov, A. V. *J. Controlled Release*

- 2001**, *73*, 401–416. (e) Ogris, M.; Wanger, E. *Drug Discovery Today* **2002**, *7*, 479–485. (f) Wolff, J. A. *Nat. Biotechnol.* **2002**, *20*, 768–769.
- (a) Wu, G. Y.; Wu, C. H. *J. Biol. Chem.* **1987**, *262*, 4429–4432. (b) Tang, M. X.; Redemann, C. T.; Szoka, F. C. *Bioconjugate Chem.* **1996**, *7*, 703–714. (c) Lim, Y.-B.; Choi, Y. H.; Park, J.-S. *J. Am. Chem. Soc.* **1999**, *121*, 5633–5639. (d) Niidome, T.; Urakawa, M.; Sato, H.; Takahara, Y.; Anai, T.; Hatakayama, T.; Wada, A.; Hirayama, T.; Aoyagi, H. *Biomaterials* **2000**, *21*, 1811–1819. (e) Bronich, T. K.; Nguyen, H. K.; Eisenberg, A.; Kabanov, A. V. *J. Am. Chem. Soc.* **2000**, *122*, 8339–8343. (f) Lynn, D. M.; Anderson, D. G.; Putnam, D.; Langer, R. *J. Am. Chem. Soc.* **2001**, *123*, 8155–8156.
- Tang, M. X.; Szoka, F. C. *Gene Ther.* **1997**, *4*, 823–832.
- Zabner, J.; Fasbender, A. J.; Moninger, T.; Poellinger, K. A.; Welsh, M. J. *J. Biol. Chem.* **1995**, *270*, 18997–19007.
- Xu, Y.; Szoka, F. C. *Biochemistry* **1996**, *35*, 5616–5623.
- Rensen, P. C.; Sliedregt, L. A.; Ferns, M.; Kieveit, E.; van Rossenberg, S. M.; van Leeuwen, S. H.; van Berkel, T. J.; Biessen, E. A. *J. Biol. Chem.* **2001**, *276*, 37577–37584.
- For polyamine-DNA complexes of defined stoichiometry, see, for example: Kabanov, A. V.; Kabanov, V. A. *Bioconjugate Chem.* **1995**, *6*, 7–20.
- Blessing, T.; Remy, J.-S.; Behr, J.-P. *Proc. Natl. Acad. Sci. U.S.A.* **1998**, *95*, 1427–1431.
- Blessing, T.; Remy, J.-S.; Behr, J.-P. *J. Am. Chem. Soc.* **1998**, *120*, 8519–8520.
- Bettinger, T.; Remy, J.-S.; Erbacher, P. *Bioconjugate Chem.* **1999**, *10*, 558–561.
- Jaaskelainen, I.; Monkkonen, J.; Urtti, A. *Biochim. Biophys. Acta* **1994**, *1195*, 115–123.
- Felgner, P. L.; Tsai, Y. J.; Sukhu, L.; Wheeler, C. J.; Manthorpe, M.; Marshall, J.; Cheng, S. H. *Proc. Natl. Acad. Sci. U.S.A.* **1987**, *84*, 7413–7417.
- Labat-Moleur, F.; Steffan, A. M.; Brisson, C.; Perron, H.; Feugeas, O.; Furstemberger, P.; Oberling, F.; Brambilla, E.; Behr, J.-P. *Gene Ther.* **1996**, *3*, 1010–1017.
- Boussif, O.; Lezoualc'h, F.; Zanta, M. A.; Mergny, M. D.; Scherman, D.; Demeinex, B.; Behr, J.-P. *Proc. Natl. Acad. Sci. U.S.A.* **1995**, *92*, 7297–7301.
- (a) Fujimoto, T.; Shimizu, C.; Hayashida, O.; Aoyama, Y. *J. Am. Chem. Soc.* **1997**, *119*, 6676–6677. (b) Fujimoto, T.; Shimizu, C.; Hayashida, O.; Aoyama, Y. *J. Am. Chem. Soc.* **1997**, *119*, 6601–6602. (c) Fujimoto, T.; Miyata, T.; Aoyama, Y. *J. Am. Chem. Soc.* **2000**, *122*, 3558–3559.
- Hayashida, O.; Kato, M.; Akagi, K.; Aoyama, Y. *J. Am. Chem. Soc.* **1999**, *121*, 11597–11598.
- Hayashida, O.; Mizuki, K.; Akagi, K.; Matsuo, A.; Kanamori, T.; Nakai, T.; Sando, S.; Aoyama, Y. *J. Am. Chem. Soc.* **2003**, *125*, 594–601.
- Hayashida, O.; Matsuo, A.; Aoyama, Y. *Chem. Lett.* **2001**, 272–273.
- For partial saccharide modification of cationic vectors, see, for example: Zanta, M.-A.; Boussif, O.; Adib, A.; Behr, J.-P. *Bioconjugate Chem.* **1997**, *8*, 839–844 and references therein.
- For polynucleotide/polysaccharide interactions, see: (a) Sakurai, K.; Shinkai, S. *J. Am. Chem. Soc.* **2000**, *122*, 4520–4521. (b) Sakurai, K.; Mizu, M.; Shinkai, S. *Biomacromolecules* **2001**, *2*, 641–650.
- Yield, 72%; mp 118–120 °C (deg). Found: C, 51.84; H, 7.62; N, 2.80. Calcd for C₁₈₄H₃₁₂N₈O₉₆·4H₂O: C, 52.07; H, 7.60; N, 2.64.
- The micrographs shown in Figure 2 are highly reproducible and representative, and especially the characteristic contrast in Figure 2d is not affected by the difference in stainings, uranyl acetate, or sodium phosphotungstate (see Supporting Information Figure S1).
- Hayashida, O.; Shimizu, C.; Fujimoto, T.; Aoyama, Y. *Chem. Lett.* **1998**, 13–14.
- For detailed analysis of the 1b-Na₂HPO₄ interaction, see ref 19.
- Preliminary results indicate that glycoviral particles undergo further self-aggregation in a saccharide-dependent manner. Maltose-derived compound 1b, for example, leads to larger particles (~280 nm) which exhibit only a considerably diminished transfection ability.
- (a) Olenyuk, B.; Whiteford, J. A.; Fechtenkotter, A.; Stang, P. J. *Nature* **1999**, *398*, 796–799. (b) Olenyuk, B.; Levin, M. D.; Whiteford, J. A.; Shield, J. E.; Stang, P. J. *J. Am. Chem. Soc.* **1999**, *121*, 10434–10435. (c) Orr, G. W.; Barbour, L. J.; Atwood, J. L. *Science* **1999**, *285*, 1049–1052. (d) Takeda, N.; Umemoto, K.; Yamaguchi, K.; Fujita, M. *Nature* **1999**, *398*, 794–796. (e) Caulder, D. L.; Raymond, K. N. *Acc. Chem. Res.* **1999**, *32*, 975–982. (f) Rivera, J. M.; Martín, T.; Rebek, J., Jr. *Science* **1998**, *279*, 1021–1023.
- (a) Stupp, S. I.; LeBonheur, V.; Walker, K.; Li, L. S.; Huggins, K. E.; Keser, M.; Amstutz, A. *Science* **1997**, *276*, 384–389. (b) Percec, V.; Ahn, C.-H.; Ungar, G.; Yearley, D. J. P.; Möller, M.; Sheiko, S. S. *Nature* **1998**, *391*, 161–164. (c) Cornelissen, J. J. L. M.; Fischer, M.; Sommerdijk, N. J. A. M.; Nolte, R. J. M. *Science* **1998**, *280*, 1427–1430. (d) Hirschberg, J. H. K. K.; Brunsvelde, L.; Ramzi, A.; Vekemans, J. A. J. M.; Sijbesma, R. P.; Meijer, E. W. *Nature* **2000**, *407*, 167–170.

JA029608T